Reactions and phase relations in the Ti-Al-O system

Acta metall. mater. Vol. 40, No. 11, pp. 3149–3157, 1992
Printed in Great Britain.

0956-7151/92 $5.00 + 0.00

REACTIONS AND PHASE RELATIONS IN THE Ti–Al–O SYSTEM

X. L. LI[1], R. HILLEL[2], F. TEYSSANDIER[2], S. K. CHOI[3] and F. J. J. VAN LOO[3]

[1]Laboratoire de Physicochimie minérale 1, CNRS-URA 116, Université Claude Bernard, F-69622 Villeurbanne Cedex, France, [2]IMP-CNRS, Université de Perpignan, F-66860 Perpignan, France and [3]Laboratory of Solid State Chemistry and Material Science, University of Technology, 5600 MB Eindhoven, The Netherlands

(Received 9 December 1991; in revised form 6 February 1992)

Abstract—Reactions between titanium and alumina were studied experimentally for Al_2O_3 substrates with a titanium-based coating and for planar Ti–Al_2O_3 diffusion couples in the temperature range between 800 and 1100°C. Isothermal sections through the phase diagram were determined by using these results as well as by investigating equilibrated alloys. These experimental sections agree with those calculated from thermodynamic data. The morphology and layer thickness of the observed reaction zones have been explained on the basis of these phase relations, making use of diffusion data from the binary systems Ti–O and Ti–Al. The important role of the initial Ti thickness on the type of reaction products has been demonstrated.

Résumé—Les réactions entre titane et alumine sont étudiées expérimentalement à partir de substrats d'alumine recouverts d'une couche à base de titane par CVD réactive, ou à partir de couples de diffusion plans Ti–Al_2O_3 recuits dans la gamme de température 800–1100°C. Des sections isothermes de ces diagrammes de phase sont déterminées à partir de ces résultats de même qu'en utilisant des mélanges de poudres à l'équilibre après traitement thermique. Ces résultats sont en bon accords avec les résultats du calcul thermodynamique. Les morphologies ainsi que les épaisseurs des domaines d'interaction sont expliquées à partir des relations entre les phases à l'équilibre et grâce aux données concernant la diffusion de systèmes binaires Ti–O et Ti–Al. L'importance de l'épaisseur initiale de titane sur la nature des phases formées est également démontrée.

Zusammenfassung—Die Reaktionen zwischen Titan und Aluminiumoxid werden experimentell an Al_2O_3-Substraten mit einem Überzug auf Titanbasis und an ebenen Ti–Al_2O_3-Diffusionspaaren im Temperaturbereich zwischen 800 und 1100°C untersucht. Isotherme Schnitte durch das Phasendiagramm werden aus diesen Ergebnissen abgeleitet und außerdem mit der Untersuchung der im Gleichgewicht stehenden Legierungen bestimmt. Diese experimentellen Schnitte stimmen mit den aus thermodynamischen Daten berechneten überein. Morphologie und Schichtdicke der beobachteten Reaktionszonen werden auf der Grundlage dieser Phasenzusammenhänge erklärt, wobei Diffusionsdaten der binären Systeme Ti–O und Ti–Al benutzt werden. Der wichtige Einfluß der anfänglichen Ti-Schichtdicke auf die entstehenden Reaktionsprodukte wird dargelegt.

1. INTRODUCTION

Because of the increasing importance of ceramic–metal combinations for high temperature applications, like in composites or in the joining and coating technology, a better understanding of their mutual interaction is necessary. It would especially be fruitful if these interactions could be predicted from the more or less easily accessible data on the relevant phase diagrams and on the diffusivities in the binary systems which are involved.

For a number of relatively simple metal–ceramic combinations with Cell-defined stoichiometric compounds such predictions turned out to be possible by using a model developed by Van Loo *et al.* [1, 2]. The principle is shown in Fig. 1. The key idea is the impossibility for atoms or ions to intrinsically diffuse into a direction where its own chemical activity is increased. It might be worthwhile to stress at this point the word "intrinsically". The equations for the *inter*diffusional fluxes in a ternary diffusion couple are dependent on the chemical potential gradients of two components. The *intrinsic* flux of a component, measured in the Kirkendall frame of reference, depends only upon its own potential gradient as shown by Lane and Kirkaldy [3]. Since the relative values of the chemical activities in simple ternary systems can be found from the slopes of the lines, important conclusions can be drawn *a priori* concerning the sequence of the compounds formed during the reaction in a diffusion couple.

For the case of Fig. 1(b), for example, the layer sequence A|AX|B|BX is excluded because of the fact, that species X then should diffuse from BX through the phase B towards the phase AX where its chemical activity is higher than in BX. This process is thermo-

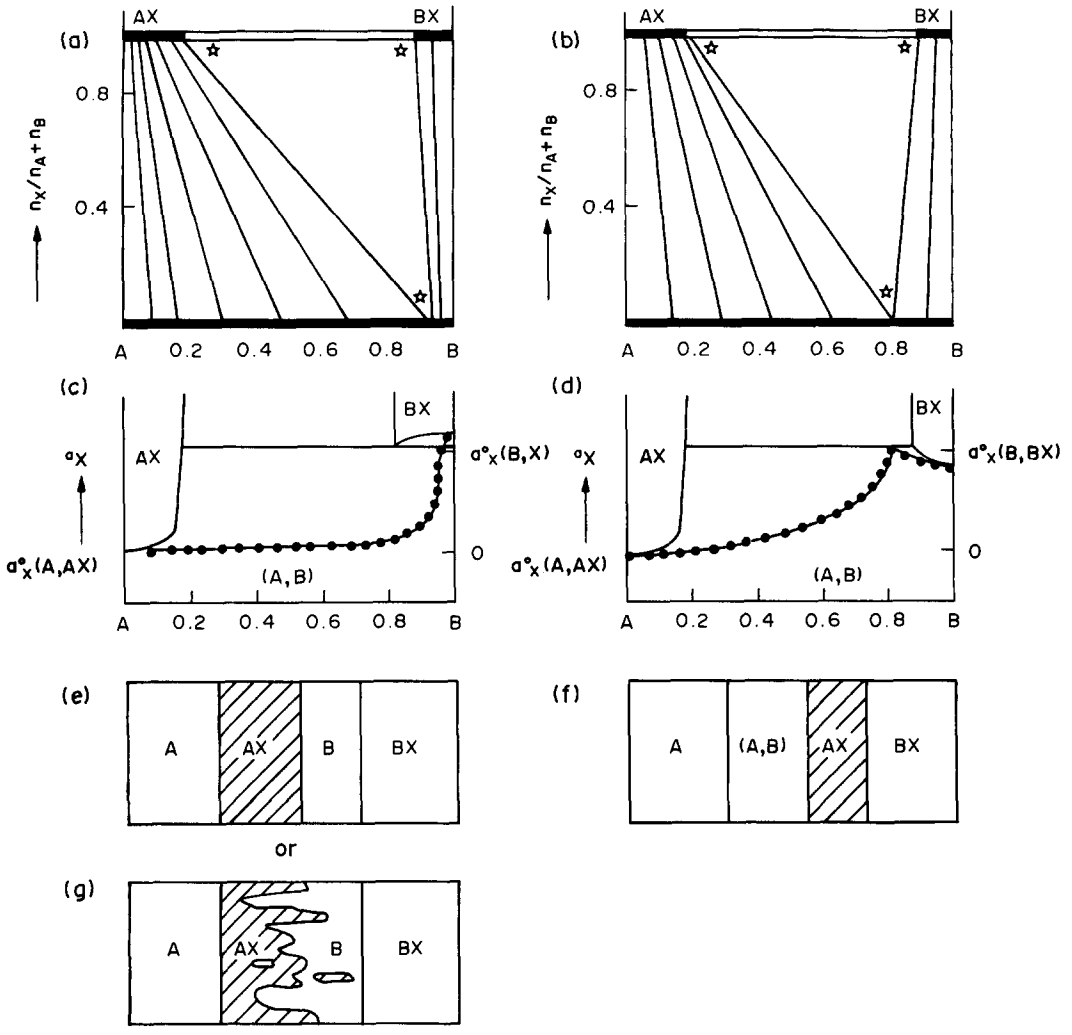

Fig. 1. (a,b) Phase relations in the A–B–X system in a rectangular configuration. (c,d) The activity of X as a function of the metal mole ratio. The dots represent the activity of X in a saturated solid solution (A,B). (e,f,g) Basic morphologies for the reaction zone in the displacement reaction $A + BX \rightarrow B + AX$ (see Refs [1, 4]).

dynamically not allowed. In the case of Fig. 1(a), no sequence is excluded on thermodynamic grounds. The diffusion kinetics determine the morphology of the reaction layer. Using Rapp's criterion [4] one may predict whether two single-phase layers or one two-phase layer is formed.

It seemed interesting to us to verify, whether such a simple model also can be applied to systems in which the phase diagram is more complicated, especially in systems where large regions of solid solutions are formed instead of stoichiometric line-compounds. We chose a study into the Ti–Al–O system, reported here, and the Ti–Si–O system on which we will report separately. Both systems are interesting from a technological point of view, especially in composite materials [5, 6] and in metal–ceramic joining [7, 8]. A literature search into the reaction between Ti and Al_2O_3 and into the Ti–Al–O phase diagram revealed a number of often conflicting results [9–17]. For instance, using infinite or finite diffusion couples, various sequences of layers were proposed:

$Ti/\alpha\text{-}Ti(O)/Ti_3Al/Al_2O_3$ [11];

$Ti/Ti_3Al/TiO/Al_2O_3$ [12];

$\alpha\text{-}Ti(O,Al)/TiAl(O)/Al_2O_3$ [13];

$Ti/Ti_3Al(O)/TiAl(O)/Al_2O_3$ [14];

$\alpha\text{-}Ti(O)/Ti_3Al(O)/Al_2O_3$ [17].

It is shown in this paper that these differences partly originate from the different thicknesses of the titanium end member (thin coatings or thick slices) and that the actual phenomena can readily be explained (and predicted) from the isothermal section through the ternary phase diagram.

2. EXPERIMENTAL

2.1. Diffusion couple preparation

Ti–Al_2O_3 diffusion couples were prepared in two ways, viz. by applying titanium-based coatings on sintered alumina or single-crystalline sapphire by gaseous cementation and by hot-pressing polished slices of titanium and alumina in a vacuum furnace.

In the first method, plane alumina substrates [sintered alumina 99.7 wt% or $(1\bar{1}02)$ cleaved sapphire crystals, dimensions 10:10:1 mm] were treated by reactive CVD in closed silica capsules, filled with thin titanium foils and HCl. The HCl concentration was equal to 1.07×10^{-5} mol · cm^{-3} and the quantity of titanium corresponded to an atomic ratio Ti/Cl = 100. The capsules were sealed and annealed in the range of 600–800°C during 0.25–200 h. We have shown [6] that at these temperatures the gaseous phase consisted of a mixture of $TiCl_4$, $TiCl_3$ and H_2. In this way titanium was transported to the alumina substrate and reacted to a coating with two distinct layers, arranged as α-Ti(O,Al)/$Ti_3Al(O)$/Al_2O_3. The thickness and exact composition of these layers depended on the experimental conditions [5, 6].

For the hot pressed diffusion couples, 10 mm diameter discs of sintered alumina (99.9 wt%) and titanium (99.8 wt%) were pressed together using a uniaxial pressure of 4 MPa in the centre of a hot chamber which was evacuated to 10^{-3} Pa. They were heated during $\frac{1}{2}$ h at 900°C, and then wrapped in Ta-foil, annealed in an evacuated silica capsule in a tube furnace at 1100°C and quenched after 72 or 140 h. Parallel with these methods, a direct joint was made in a vacuum furnace (10^{-4} Pa vacuum, uniaxial pressure 0.2 MPa) at 100°C for 50 and 100 h. The thickness of the alumina disc was 1 mm, the thickness of the titanium disc varied between 0.025 mm (for making a completely finite equilibrated couple) and 4 mm (for making semi-infinite couples). For further experimental details see Ref. [8].

2.2. Determination of isothermal sections of the phase diagram

Homogeneous alloys were made in two ways, viz. by sintering powder mixtures of titanium and alumina or aluminium and TiO_2. The Ta-wrapped pellets were placed in an alumina crucible, which was annealed in an evacuated silica capsule at 800 and 1000°C until equilibrium was reached. The same was done in the binary Ti–O system by mixing six powder samples consisting of different amounts of Ti and Ti_2O and for the Ti–Al system by mixing Ti and Al powders at four compositions between 10 and 35 at.% Al. For more experimental details see Ref. [6].

The powder metallurgy method has the serious disadvantage of containing an unknown amount of extra oxygen which adsorbs at the large powder surface. Therefore, arc-melting of mixtures composed of titanium lumps and alloys of the starting composition Ti_2O_3, Ti_3Al or TiAl was also carried out. The alloys were then homogenised at 1100°C. The analyses of the annealed diffusion couples were also used for the determination of the phase diagram.

2.3. Analyses of alloys and diffusion couples

Both the alloys and the diffusion couples have been analysed by light microscopy, scanning electron microscopy (SEM), electron probe microanalysis (EPMA) and by X-ray diffraction.

By light microscopy and SEM, the various phases of importance for our investigation [α-Ti(O,Al), β-Ti(O,Al), $Ti_3Al(O)$, TiAl, TiO and Al_2O_3] were readily distinguished after etching with a 2% HF, 2% HNO_3 aqueous solution. The quantitative analysis by EPMA, however, turned out to be very intricate and time-consuming because of the unavoidable presence of thin oxide surface films on the alloys which tend to higher apparent oxygen contents.

In order to take this thin film into account, the EPMA measurements were performed at various excitation voltages from 2 to 20 kV with a beam current of 10 nA, using Ti-L_α radiation below 7 kV. The standards were pure titanium and aluminium and Fe_2O_3 for oxygen. Using the PROZA and the thin-film programs of Bastin [18, 19] we were able to measure the actual bulk composition of the alloys and in the diffusion couple cross sections as well as the thickness and composition of the surface films. In the composition range of interest, the Ti/Al molar ratio was not affected by the presence of the oxide film.

We made use of this fact by developing a combined X-ray diffraction and SEM equipped with energy dispersive spectroscopy (EDS) analysis to determine the composition of especially, the α-Ti(O,Al) and $Ti_3Al(O)$ solid solutions. Using literature data [20, 21] and our own X-ray measurements on binary Ti–O and Ti–Al alloys [6], we constructed a set of calibration curves for the volume of the lattice cell vs the amount of oxygen or aluminium, assuming that the interstitially dissolved oxygen and the substitutionally dissolved Al do not influence their individual effect on the cell volume (Fig. 2).

To check this procedure, ternary alloys made by the powder method were analysed in this way. The weighed-in and estimated composition are in good agreement for the aluminium-poor alloys (Table 1).

3. RESULTS

The isothermal sections determined at 1000 and 1100°C were in quite close agreement. They show, as the one determined at 1100°C (Fig. 3), tie-lines radiating from Al_2O_3 to all other phases present in the diagram, except for the β-Ti solid solution which is in equilibrium with α-Ti(O,Al).

The diffusion paths (average composition measured in a diffusion couple from one end member to the other) shown in Fig. 3 for couples with thin

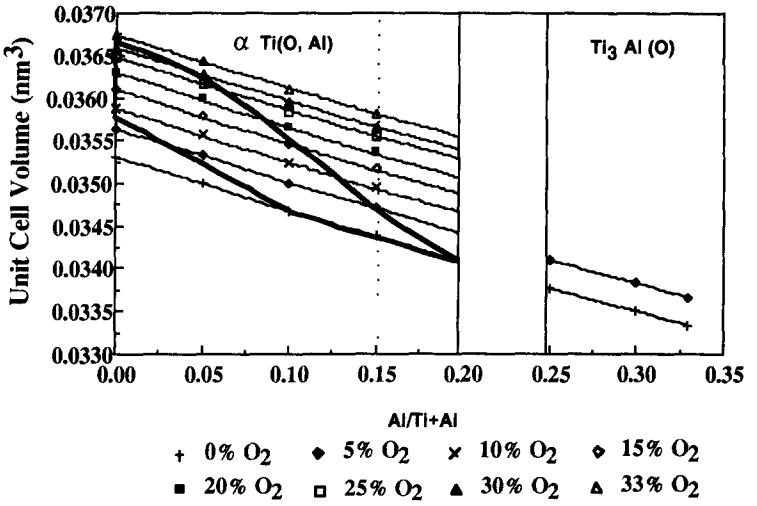

Fig. 2. Calculated volumes of the hexagonal cell of α-Ti(O,Al) and $Ti_3Al(O)$ as a function of the composition. The bold line is the estimated boundary of α-Ti(O,Al).

titanium foils all show the layer sequence Al_2O_3/$Ti_3Al(O)$/Ti_2O, where Ti_2O stands for the saturated solid solution of oxygen in α-Ti. A small amount (maximum about 5 at.% Al) was found in Ti_2O very close to the Ti_3Al layer. This sequence was found in all gaseous cemented Al_2O_3 substrates as well as in sandwich hot-pressed diffusion couples Al_2O_3/Ti/Al_2O_3 with 0.025 mm thick titanium discs as shown in Fig. 4. In infinite diffusion couples one of the end members is still pure β-Ti. The layer sequence is then found to be Al_2O_3/TiAl(O)/$Ti_3Al(O)$/α-Ti(O,Al)/β-Ti as indicated by the diffusion path in Fig. 3. In Fig. 5, two micrographs are shown of such a couple.

4. DISCUSSION

The isothermal sections found by us differ from the diagrams published by Tressler [12] (Fig. 6), especially in the phase equilibria between TiAl, Ti_3Al, α-Ti(O,Al), TiO and Al_2O_3. In order to verify whether our results were consistent with the published thermodynamic properties of the Ti–O and Ti–Al alloys we determined the phase relations at 1373 K by Gibbs free energy minimisation of the total system. Calculations were performed with the Solgasmix program taking into account the line compounds given in Table 2 and the solid solution α-Ti(O). Due to the low solubility of oxygen in β-Ti, the β-Ti(O) solid solution was not considered for the calculation.

Table 1. Comparison between the prepared and estimated composition of the α-Ti(O,Al) phase

Weighed-in composition	Measured volume of the cell (nm^3)	Estimated composition
$Ti_{0.82}O_{0.05}Al_{0.13}$	0.03515 ± 0.00002	$Ti_{0.77}O_{0.11}Al_{0.12}$
$Ti_{0.90}O_{0.06}Al_{0.04}$	0.03550 ± 0.00009	$Ti_{0.89}O_{0.07}Al_{0.04}$
$Ti_{0.87}O_{0.08}Al_{0.05}$	0.03549 ± 0.00009	$Ti_{0.87}O_{0.08}Al_{0.05}$
$Ti_{0.80}O_{0.12}Al_{0.08}$	0.03550 ± 0.0001	$Ti_{0.79}O_{0.13}Al_{0.08}$
$Ti_{0.79}O_{0.20}Al_{0.01}$	0.03628 ± 0.00004	$Ti_{0.78}O_{0.21}Al_{0.01}$

4.1. Ti–O binary phase diagram

The Gibbs free energies of formation of the Ti–O stoichiometric compounds came from Chase *et al.* [22] and are consistent with JANAF [23] and Pankratz [24]. The variation of the Gibbs free energies of the solid solution α-Ti(O) as a function of the composition at 1373 K was obtained in the following way.

The information we have about the α-Ti(O) phase is

—According to the assessed Ti–O Murray [20] phase diagram, the upper and lower phase boundary compositions of α-Ti(O) are $Ti_{0.667}O_{0.333}$ and $Ti_{0.915}O_{0.085}$.

—The corresponding free energy of formation based on the data given by Kubaschewski and Alcock [29] on the Ti–O system is
ΔG^{1373} $Ti_{0.915}O_{0.085} = -44{,}272$ J/mol
ΔG^{1373} $Ti_{0.67}O_{0.33} = -152{,}000$ J/mol.

—As a result of this boundary composition we know that the tangent to the ΔG α-Ti(O) curve for the composition $X_O = 0.33$ includes the point corresponding to ΔG $\beta Ti_{0.5}O_{0.5}$.

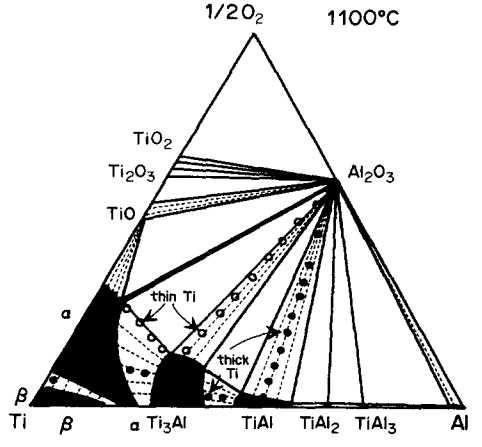

Fig. 3. Isothermal section of the Ti–Al–O phase diagram experimentally determined at 1100°C.

Fig. 4. Finite diffusion couple $Al_2O_3/Ti/Al_2O_3$ welded at 1100°C, 100 h in vac. (10^{-6} torr). Thickness ratio: $Ti_2O:Ti_3Al(O) = 1:1.46 \pm 0.13$.

Five conditions are then obtained which allow the determination of five parameters: the two coefficients of the tangent, the lattice stability of oxygen between the h.c.p. and gas state (which is not given in the literature) and two parameters (A and B) for the equation of ΔG α-Ti(O)

$$\Delta G \; Ti_{(1-X)}O_X \text{ (ref. Ti h.c.p., O h.c.p.)} = X(1-X)(AX+B).$$

Taking into account the lattice stability of titanium determined by Kaufman [26] ($G_{Ti}^{h.c.p.} - G_{Ti}^{b.c.c.} = -4351 + 3.766 \cdot T$ J/mol), the calculation gives $A = -848{,}533$, $B = -678{,}039$, $G1/2O_2^{h.c.p.} - G1/2O_2^{gas} = 201{,}456$ J/mol. The corresponding Gibbs diagram is presented in Fig. 7.

4.2. Ti–Al binary phase diagram

The Ti–Al system was first investigated by Kaufman [26] who determined the Gibbs free energy of formation of Ti_3Al, TiAl and $TiAl_3$ described as line compounds. The α- and β-Ti(Al) solid solutions were modelized as regular solutions. More recently, Murray [27] did the same calculation but included the homogeneity range of Ti_3Al and TiAl as well as order parameters, with a model which combines the sub-

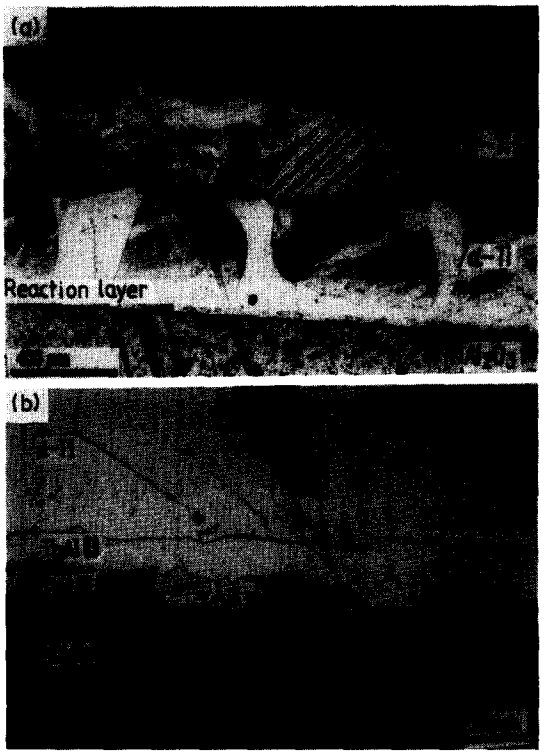

Fig. 5. Infinite diffusion couples. (a) Ti/Al_2O_3 annealed at 1100°C, 140 h in silica tube. (b) Ti/Al_2O_3 welded at 1100°C, 50 h in vac. (10^{-6} torr).

lattice description and the Bragg–Williams approximation. The Ti–Al system has also been studied by Gros *et al.* [28] but the calculation involves only the Ti-rich corner which includes liquid, b.c.c., h.c.p. and Ti_3Al phases.

The calculation of Murray is one of the most recent and complete but does not take into account $TiAl_2$, whose existence seems now to be well established. We have thus undertaken a new calculation based on the data of Murray [27] for $TiAl_3$ and the α- and β-Ti(Al) solid solutions and including $TiAl_2$. We were not able to use the Gibbs free energy of $TiAl_2$ established by Kaufman [26] which is too high according to the data of Murray. Our own estimation of this value at 1373 K is: ΔG^{1373} $Ti_{0.33}Al_{0.67} = -26{,}000$ J/mol.

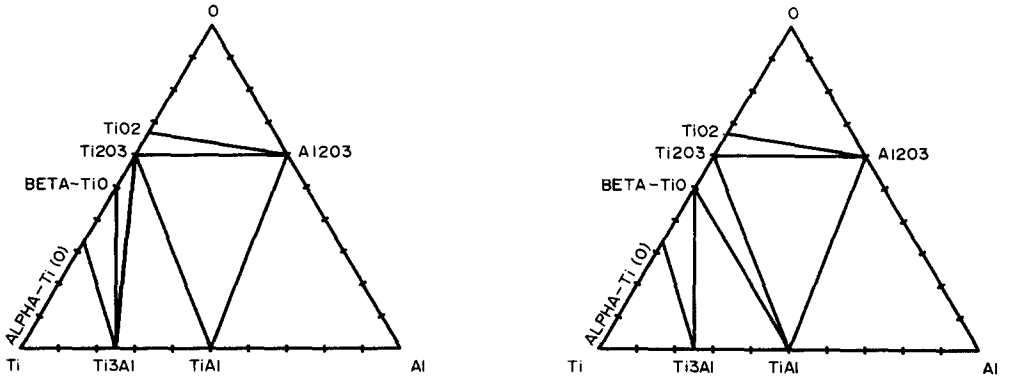

Fig. 6. The two possible phase diagrams at 870°C according to Tressler *et al.* [12].

Table 2. Gibbs free energy of formation of the line compounds, taken into account in our calculations

Line compounds	ΔG (J/mol) 1373 K
1/2 βTiO	−205,907
1/5 Ti_2O_3	−229,223
1/8 Ti_3O_5	−232,032
1/11 Ti_4O_7	−231,664
1/3 TiO_2 rutile	−231,994
1/4 Ti_3Al	−18,377
1/2 TiAl	−26,165
1/3 $TiAl_2$	−26,000
1/4 $TiAl_3$	−23,007

We used a polynomial expansion for the excess Gibbs free energy of Ti_3Al and TiAl in their homogeneity range

Ti_3Al (ref. Ti h.c.p., Al h.c.p.)

$$\Delta G = X_{Al} \cdot (1 - X_{Al}) \cdot (C \cdot X_{Al} + D)$$

TiAl (ref. Ti f.c.c., Al f.c.c.)

$$\Delta G = X_{Al} \cdot (1\text{-}X_{Al}) \cdot (L \cdot X_{Al}^2 + M \cdot X_{Al} + N).$$

The results of the calculation have to be in accordance with the phase boundaries of the assessed binary Ti–Al phase diagram at 1373 K. Eight conditions can then be determined which allow the determination of the five parameters of the excess Gibbs free energy of Ti_3Al and TiAl, as well as the equations of the common tangents to α-Ti(Al) and Ti_3Al, and TiAl and $TiAl_2$. The following lattice stability of titanium and aluminium established by Kaufman [26] was used

$$G_{Ti}^{h.c.p.} - G_{Ti}^{b.c.c.} = -4351 + 3.766 \cdot T \text{ J/mol}$$

$$G_{Ti}^{f.c.c.} - G_{Ti}^{b.c.c.} = -1004 + 3.766 \cdot T \text{ J/mol}$$

$$G_{Al}^{h.c.p.} - G_{Al}^{liq} = -5230 + 9.707 \cdot T \text{ J/mol}$$

$$G_{Al}^{f.c.c.} - G_{Al}^{liq} = -10{,}740 + 11.506 \cdot T \text{ J/mol.}$$

The calculated parameters of the polynomial expansion for the excess Gibbs free energy of Ti_3Al and TiAl expressed in J/mol are

$$C = -31{,}162,\ D = -70{,}059$$

$$L = 77{,}644,\ M = -157{,}365,\ N = -32{,}187.$$

The resulting free energy diagram at 1373 K is given in Fig. 8.

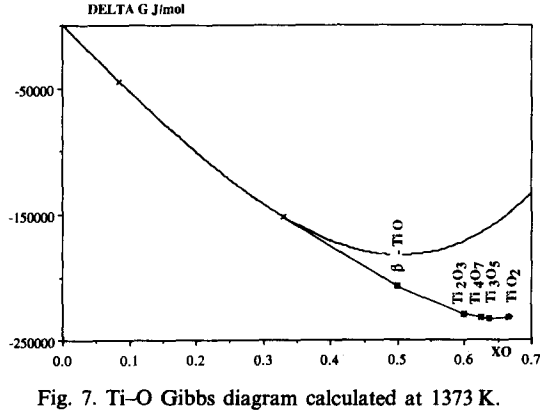

Fig. 7. Ti–O Gibbs diagram calculated at 1373 K.

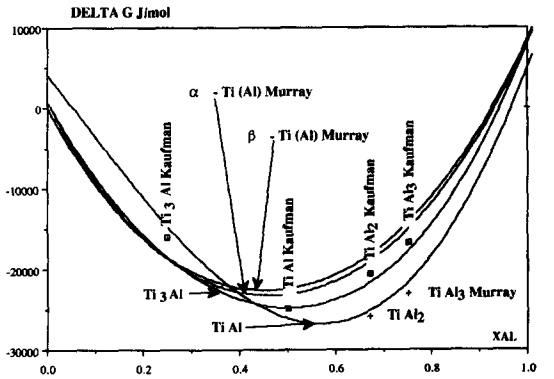

Fig. 8. Ti–Al Gibbs diagram calculated at 1373 K. Comparison with data calculated by Murray [27] and by Dew-Hugues and Kaufman [26].

When using these data for the calculation of the isothermal section of the ternary Ti–Al–O phase diagram, tie lines between TiAl and the saturated α-Ti(O) solid solution or β-TiO are obtained instead of the tie line between Al_2O_3 and Ti_3Al as experimentally observed. Two remarks should be made concerning these differences. Firstly, the accuracy of the used free energy values for the compounds is not very high. This is important especially because the free energy values of a reaction in this system are dominated by the much larger values for the oxides compared with the aluminides (see Table 2). Secondly, the solubility of oxygen in Ti_3Al and TiAl, which is suspected to involve a large variation of the free energy value, is neglected.

In order to cope with this diffculty we undertook a new calculation including the solubility of oxygen in Ti_3Al and TiAl. A sublattice model would be suitable for taking into account both the solubility of oxygen and the homogeneity range of the intermetallic compounds. However, due to the lack of information at temperatures other than 1373 K, we focused on the influence of oxygen on Ti_3Al and TiAl considered as line compounds using a simpler model. The Gibbs free energy of Ti_3Al and TiAl were obtained from our previous model

$$\Delta G\ Ti_{0.75}Al_{0.25} = -18{,}377 \text{ J/mol}$$

$$\Delta G\ Ti_{0.50}Al_{0.50} = -26{,}165 \text{ J/mol.}$$

The solubility of oxygen is described by a quasi-binary approximation between Ti_3Al or TiAl and O

$$G^{h.c.p.} = (1 - X_O)G_{Ti0.67Al0.33} + X_O\ G_O + RT[X_O \ln X_O + (1 - X_O) \ln (1 - X_O)] + {}^{XS}G^{h.c.p.}$$

where

$${}^{XS}G^{h.c.p.} = \lambda X_O(1 - X_O)$$

λ is the excess parameter of the solid solution described with a regular model. The lattice stability of

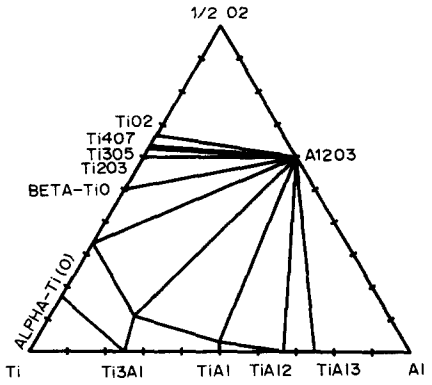

Fig. 9. Isothermal section of the Ti–Al–O phase diagram calculated at 1373 K.

oxygen between the h.c.p. and the gas state is that determined for the Ti–O system

$$G1/2O_2{}^{\text{h.c.p.}} - G1/2O_2{}^{\text{gas}} = 201{,}456\ \text{J/mol}.$$

The lattice stability of oxygen between the f.c.c. and the gas state as well as the regular parameters were adjusted to represent satisfactorily the experimentally determined limit of solubility

$$\text{Ti}_3\text{Al–O:} \quad \text{limit } X_O = 0.11 \quad \lambda = -720{,}000\ \text{J}$$

$$\text{TiAl–O:} \quad \text{limit } X_O = 0.03 \quad \lambda = -630{,}000\ \text{J}$$

$$G1/2O_2{}^{\text{f.c.c.}} - G1/2O_2{}^{\text{gas}} = 230{,}120\ \text{J/mol}.$$

The calculated isothermal ternary section at 1373 K is given in Fig. 9. If we exclude the Ti rich corner where the α- or β-Ti(O,Al) solid solutions were not taken into account, this diagram agrees very well with the experimental one. These results emphasize the fact that a strong variation of the free energy is induced by the solubility of oxygen

$$\text{Ti}_{0.75}\text{Al}_{0.25}: \quad \Delta G = -18{,}377\ \text{J/mol}$$

$$\text{Ti}_{0.668}\text{Al}_{0.222}\text{O}_{0.11}: \quad \Delta G = -68{,}272\ \text{J/mol}$$

$$\text{Ti}_{0.50}\text{Al}_{0.50}: \quad \Delta G = -26{,}165\ \text{J/mol}$$

$$\text{Ti}_{0.485}\text{Al}_{0.485}\text{O}_{0.03}: \quad \Delta G = -39{,}837\ \text{J/mol}.$$

In the case of TiAl–O this variation represents an increase of more than 50% of ΔG for only 3% oxygen dissolved. For $Ti_3Al(O)$ the free energy value at 11% oxygen is more than three times the initial value.

If we accept the experimentally determined isothermal section to be correct, we can construct from them the rectangular sections shown in Fig. 10(a) and (b), and we can estimate the corresponding plots of ln a_O and ln a_{Al} shown in Fig. 10(c).

These estimates are based on the thermodynamic data in Table 2, on the data given by Kubaschewski [29] on the Ti–O system which takes into consideration the solid solubility range of TiO and on the data of the above mentioned thermodynamic calculation. We now use Fig. 10 (c) and (d) as a starting point for our prediction of the diffusion path in a semi-infinite Ti–Al_2O_3 couple.

Figure 10(d), for instance, forbids a layer sequence Al_2O_3/TiO/Ti_3Al/α/β-Ti, suggested by Tressler [12], since then Al has to diffuse from Al_2O_3 through a minimum activity in TiO to a higher activity in Ti_3Al, which is thermodynamically impossible.

Figure 10(c) forbids a diffusion path of the type Al_2O_3/$TiAl_3$/$TiAl_2$/TiAl/Ti_3Al/α-Ti(O,Al)/β-Ti. The reason is that since the activity of oxygen has to decrease going from the Al_2O_3/$TiAl_3$ boundary (ln $a_O \approx -75$) towards the α-solid solution. Such a low activity of oxygen in α means a negligible concentration of oxygen and that is in conflict with the mass balance, since the oxygen amount which diffuses away from Al_2O_3 must be 3/2 times the amount of aluminium atoms. The sequence Al_2O_3/α/Ti_3Al/α/β-Ti is, from Fig. 10(c) and (d) not necessarily forbidden, but very unlikely since between very small limits in the activities of oxygen and aluminium the path would then enter, leave and re-enter the α-phase. No problem is offered with a sequence of the type

$$Al_2O_3/TiAl/Ti_3Al/\alpha/\beta\text{-Ti}$$

or

$$Al_2O_3/Ti_3Al/\alpha/\beta\text{-Ti}$$

indicated in Fig. 3. Which of these paths will be followed depends, in fact, on the relative ratio of the diffusivities in the TiAl, Ti_3Al and α-Ti(O,Al) phases. The diffusion of oxygen in α-Ti is fast [30], that of Al in Ti_3Al or α-Ti is low [31]. In order to let oxygen diffuse freely into α-Ti and to cope with the mass balance, the formation of TiAl has to be expected and is indeed found. If, on the other hand, the initial Ti thickness is small, then the amount of oxygen which enters Ti is small and the titanium becomes rapidly saturated in oxygen, consequently leading to a change in diffusion path. This path no longer starts at the pure titanium, but at a more or less saturated solid solution α-Ti(O). During this process, TiAl formed in the beginning of the process, will react with the unsaturated α-Ti(O) solution of e.g. composition $Ti_{8/3}O$ according to a reaction scheme of the type

$$12\ \text{Ti} + Al_2O_3 \rightarrow 3\ Ti_{8/3}O + Ti_3Al(O) + TiAl(O) \quad (1)$$

$$3\ Ti_{8/3}O + TiAl(O) \rightarrow 3\ Ti_2O + Ti_3Al(O) \quad (2)$$

$$12\ \text{Ti} + Al_2O_3 \rightarrow 2\ Ti_3Al(O) + 3\ Ti_2O \quad (3)$$

The limited thickness of the Ti_3Al layer permits its formation from a diffusion point of view. If the reaction given above is represented according to the actual measured average compositions for the thin-foiled Ti–Al_2O_3 couple, one gets

$$10.2\ \text{Ti} + Al_2O_3 \rightarrow 7.9\ Ti_{0.680}Al_{0.238}O_{0.082} + 7.29\ Ti_{0.662}Al_{0.016}O_{0.322}. \quad (4)$$

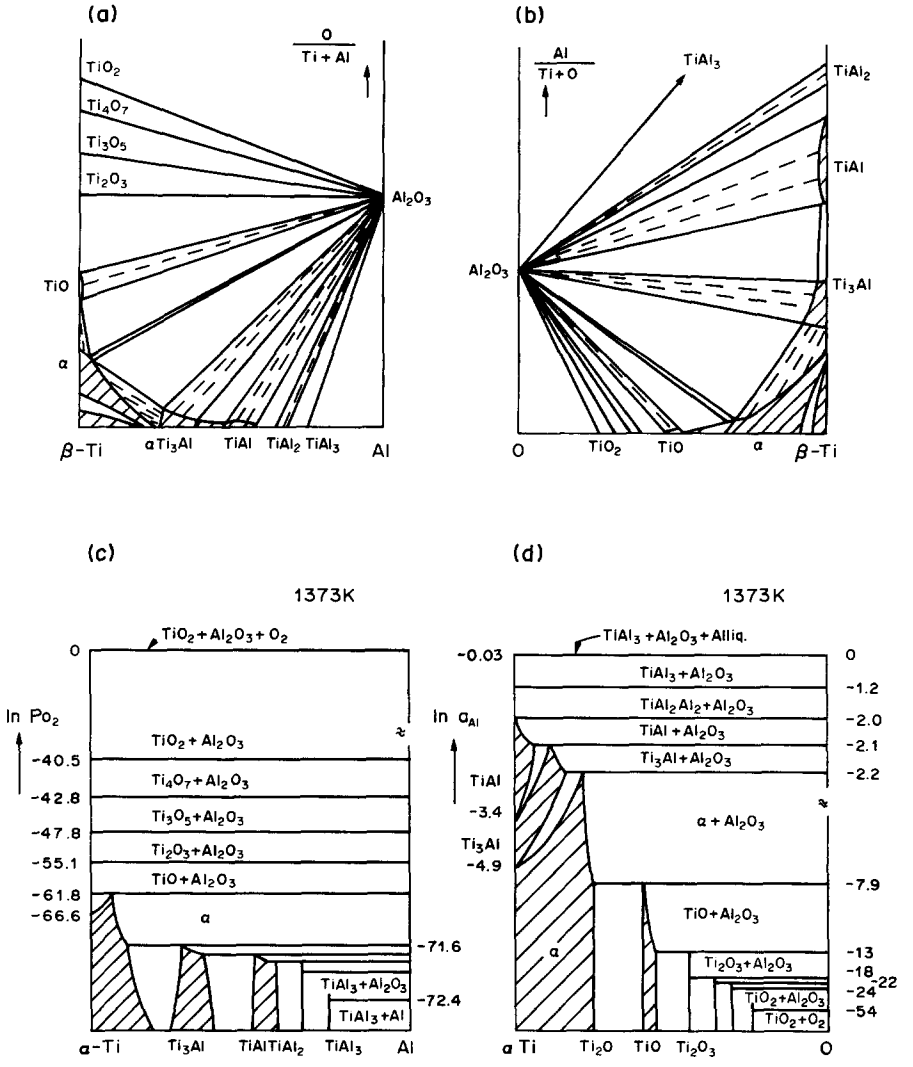

Fig. 10. Activities data plotted as a function of composition.

The cell volumes (per atom) of the $Ti_3Al(O)$ and α-Ti(O) phases are calculated from Fig. 2 as shown in Table 3. That means, that according to reaction (4) the thickness ratio of the two layers has to be

$$Ti_3Al(O):\alpha - Ti(O)$$
$$= (0.0156 \times 7.9)/(0.0124 \times 7.29) \text{ i.e. } 1.36:1$$

which is in excellent agreement with the value of 1.39 ± 0.12, experimentally found as shown in Fig. 4. This, in fact, is also an independent confirmation of the composition measurements by EPMA.

5. CONCLUSION

By different experimental techniques a consistent isothermal section of the Ti–Al–O phase diagram has been established in the range 1000–1100°C. From this section, together with estimated thermodynamic data, it is possible to explain in detail the layer sequence and morphology in diffusion couples Al_2O_3–Ti. The same method can, therefore, fruitfully be used to predict the diffusion processes and layer morphologies in this type of system. This will be shown in a future paper dealing with the interaction between SiO_2 and Ti.

Table 3. The number of atoms per unit cell is equal to the number of Ti + Al atoms (which is 2) plus the number of interstitially dissolved oxygen atoms [which e.g. for the composition $Ti_{0.680}\ Al_{0.238}\ O_{0.082}$ is equal to $2 \cdot (0.082)/(1 - 0.082)$]

Composition	Unit cell volume (nm^3) (Fig. 2)	Number of at./cell	Volume per atom nm^3/at.
$Ti_{0.680}\ Al_{0.238}\ O_{0.082}$	0.0341	2.179	0.0341/2.179 = 0.0156
$Ti_{0.662}\ Al_{0.016}\ O_{0.322}$	0.0366	2.949	0.0366/2.949 = 0.0124

REFERENCES

1. F. J. J. Van Loo, J. A. Van Beek, G. F. Bastin and R. Metselaar, *Diffusion in Solids: Recent Developments* (edited by M. A. Dayananda and G. E. Murch), pp. 231–259. TMS (1985).
2. F. J. J. Van Loo, *Prog. Solid St. Chem.* **20,** 47 (1990).
3. J. E. Lane and J. S. Kirkaldy, *Can. J. Phys.* **42,** 1643 (1964).
4. R. A. Rapp, A. Ezis and G. J. Yurek, *Metall. Trans.* **4,** 1283 (1973).
5. R. Hillel, J. C. Viala, X. L. Li and J. Bouix, *Proc. of the VII European Meeting on Chemical Vapor Deposition* (edited by M. Ducarroir, C. Bernard and L. Vandenbulke), Colloque de Physique C5, *J. Physique* **50,** 9450 (1989).
6. X. L. Li, Thèse de Doctorat, Lyon (1990).
7. S. K. Choi, F. J. J. Van Loo and R. Metselaar, *Proc. of the 7th CIMTEC* (edited by P. Vincenzini), pp. 633–640 (1990).
8. S. K. Choi, Ph. D. thesis, K. U. Leuven (1989).
9. C. P. Lofton and W. E. Swartz, *Thin Solid Films* **52,** 271 (1978).
10. Y. S. Chaug, N. J. Chou and Y. H. Kim, *J. Vac. Sci. Technol. A* **5,** 1288 (1987).
11. G. Geschwind, *A Study of Interfacial Reactions in Titanium/Sapphire (Al_2O_3) Composites*. U.S. Nat. Tech. Inform. Serv. AD Rep. 1972, no. 747357 from Govt. Rep. Announce (U.S.), **72**(20), 108 (1972).
12. R. E. Tressler, T. L. Moore and R. L. Crane, *J. Mater. Sci.* **8,** 151 (1973).
13. M. B. Chamberlain, *J. Vac. Sci. Technol. A* **15,** 240 (1978).
14. F. Hatakeyama, K. Suganuma and T. Okamoto, *J. Mater. Sci.* **21,** 2455 (1986).
15. X. A. Zhao, E. Kolawa and M. A. Nicolet, *J. Vac. Sci. Technol. A* **4,** 3139 (1986).
16. J. H. Selverian, M. Bortz, F. S. Ohuchi and M. R. Notis *Mater. Res. Soc. Symp. Proc.* **108,** 107 (1988).
17. J. Kivilahti and E. Heikinheimo, *D. Gesellsch. f. Metallkde*, Bad Nauheim, April (1989).
18. G. F. Bastin and H. J. M. Heijligers, *Proc. of the 21st Annual Conf. of Microbeam Analysis Society* (edited by A. D. Romig and W. F. Chambers), pp. 285–288. San Francisco Press, Calif. (1986).
19. G. F. Bastin, H. J. M. Heijligers and J. M. Digkstra, *Proc. XIIth Int. Congr. f. Electron Microscopy* (edited by L. D. Peachy and D. B. Williams), Vol. 2, pp. 216–218. San Francisco Press, Calif. (1990).
20. J. L. Murray and H. A. Wriedt, *Bull. Alloy Phase Diagr.* **8,** 148 (1987).
21. J. L. Murray, *Phase Diagrams of Binary Titanium Alloys*, pp. 12–24. ASM Int., Metals Park, Ohio (1987).
22. M. W. Chase, J. L. Curnutt, H. Prophet and R. A. McDonald, *JANAF Thermochemical tables supplement, J. Phys. Chem.* Ref. Data, no. 4 (1975).
23. *JANAF Thermochemical Tables*, 2nd edn, NSRDS-NBS 37, Washington D.C. (1971).
24. L. B. Pankratz, Thermodynamic properties of elements and oxides. United States department of the Interior, Bulletin 672 (1982). J. G. Watt, secretary, Bureau of mines, R. C. Horton, director.
25. A. D. Mah, K. K. Kelley, N. L. Gellert, E. G. King and C. J. O'Brien, Report of Investigation 5316.
26. D. Dew-Hugues and L. Kaufman, *Calphad* **3,** 175 (1979).
27. J. L. Murray, *Metall. Trans.* **19A,** 243 (1988).
28. J. P. Gros, B. Sundman and I. Ansara, *Scripta metall.* **22,** 1587 (1988).
29. O. Kubaschewski and C. B. Alcock, *Metallurgical Thermochemistry*, 5th edn. Pergamon Press, Oxford (1979).
30. R. J. Wasilewski and G. L. Kehl, *J. Inst. Metals* **83,** 94 (1954–55).
31. K. Hirano and Y. Iijima, *Diffusion in Solids: Recent Developments* (edited by M. A. Dayananda and G. E. Murch), pp. 141–167. T.M.S. (1985).